

A Study on Plasma Polymerization of Acrylic Acid Using APF Plasma Focus Device

M. H. S. Alavi · M. Habibi · R. Amrollahi ·
F. Afshar Taromi

Published online: 25 December 2010
© Springer Science+Business Media, LLC 2010

Abstract The most conventional way for polymerization of acrylic acid on different substrates is using RF devices and introducing of other devices is under way. In this work we have a new study on formation of polymer Acrylic Acid using APF plasma focus device. The formation of plasma polymer acrylic acid is discussed using results obtained from attenuated total reflectance infrared spectroscopy (ATR). The results show that after 15 shots, nitrogen pulses performed polymerization on the specimens and the main peaks of ATR spectra assured poly acrylic acid formation on SBR substrate.

Keywords Plasma polymerization · APF Plasma focus device · Acrylic acid · ATR-FTIR

Introduction

Plasma polymerization is one of the well-known techniques for depositing thin layers on different substrates without affecting their bulk properties [1–3]. Generally, plasma polymerization is accomplished by introducing different types of monomer precursors (vapour or aerosol) into a plasma reactor chamber leading to the deposition of so-called plasma polymers.

Plasma polymerization is used to create unique kinds of polymers, which cannot be obtained using classical

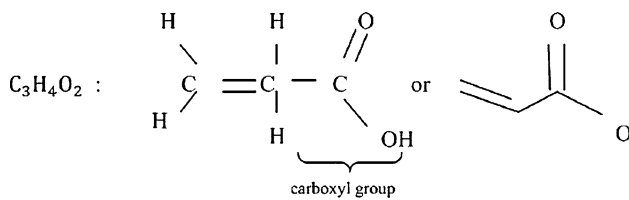
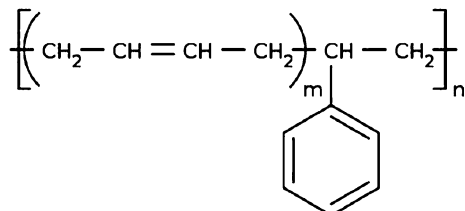
chemical polymerization processes and which significantly differ from conventional polymers. As plasma polymers are derived from the assembly of various molecular fragments produced in the plasma vapour phase, their chemical structure tends to be random and more cross-linked compared to conventional polymers. Moreover, plasma-polymerized films are generally amorphous, free from pinholes, highly resistant to heat and corrosion and very adhesive to a variety of substrates including conventional polymer, glass and metal surfaces. Owing to these excellent characteristics, plasma polymers have been used in a wide variety of applications including barrier coatings, protective coatings, selective permeation membranes, and dielectric layers in microelectronics [4].

Among them plasma polymer acrylic acid (ppAA) have gained great interest as adhesion-promoting interlayers, e.g., in carbon fiber/epoxy composites, as well as bio interphases [1]. The –COOH group in Fig. 1 plays the main role in ppAAs and the main goal in this area of research is to gain a surface with high density carboxylated surfaces which can be used for immobilization of bio-molecules, high retention of carboxylic acid groups, improving hydrophilicity and wrinkle recovery angle of some textile surfaces [1, 3].

We used SBR (Styrene-Butadiene-Rubber) (Fig. 2) as substrate and nitrogen as medium gas. Polymers, especially rubbers, require surface treatment to achieve a satisfactory level of adhesion for bonding. Treatments of different types of rubbers (Both natural and synthetic) by plasma have been studied [5]. Polymerization of Low-molecular-weight acrylic compounds is used to create an oxygen permeation barrier. Details have been given of improvements in peel strength of silicone rubber joints by plasma pre-treatment followed by grafting with acryl amide and acrylic acid. Furthermore, plasma can be used as a means of providing

M. H. S. Alavi · M. Habibi (✉) · R. Amrollahi
Fusion Lab., Amirkabir University of Technology, Tehran, Iran
e-mail: mortezahabibi@gmail.com

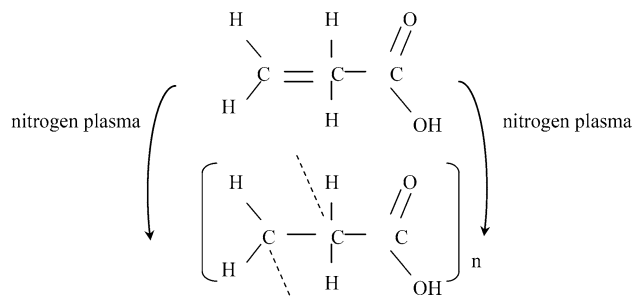
F. Afshar Taromi
Department of Polymer Engineering and Color Tech, Amirkabir University of Technology, Tehran, Iran

**Fig. 1** Chemical structure of acrylic acid**Fig. 2** Chemical structure of SBR

hydrophobicity to rubber [5]. Among them SBR is one of the most important synthetic rubbers. It accounts for about 40% of the total synthetic elastomer production [6], so it can be a good candidate for investigation in this study.

Although some other devices like DBD (Dielectric Barrier Discharge) was introduced for polymerization of acrylic acid [4], but our device characteristic is more similar to RF reactors/generators in case of pressure (both continuous and pulsed [7]) ranging from 3 to 50 Pa (23–375 mTorr) [1–3, 8–10] which are commonly used in recent studies. In order to achieve an optimal polymerization (stable polymers) and the best characteristic on different substrates in such devices, studies has been done e.g., varying input energy and gas mixture feed, duration of RF discharge and etc. to achieve the best results [1, 3].

In pulsed discharges of the plasma focus device, the accelerated current sheath forms a dense (10^{25} – 10^{26} m^{-3}) short lived ($\sim 100 \text{ ns}$), and high temperature (1–2 keV) plasma pinch column [11]. Due to $m = 0$ instability the plasma pinch is broken and the resulting induced electric field accelerates electrons and ion beams ($V \geq 10^7 \text{ cm/s}$). The details of the plasma focus device have been published earlier [12]. The energy profile of these ion beams is continuous, from a few keV to some hundred keV. High energy ion beams originating mainly from plasma focus are progressively used in material surface modification and thin film fabrication during last few years [13]. Ions coming from the focus region are much more energetic than the ions present in other materials processing reactors. These features give plasma focus great importance for generation of relatively uniform implantation profiles in materials and polymerization. The ion dose is sufficient to change the physical properties of the outer layers of the substrate. Also the energy delivered by the ion beam raises the surface temperature to a high value without noticeable changes in

**Fig. 3** Acrylic acid polymerization

the bulk temperature. This last thermal transient can induce several surface treatment processes (such as annealing of crystal lattice defects, quenching and formation of new phases) and besides it has been found that it can promote the penetration of the ions to depths well beyond the ions' normal range [14].

The ion energy spectrum basically follows a $dN/dE \sim E^{-k}$ law, where N is the number of ions with energy E , and k has a value of ~ 3.5 [15]. In order to measure the ion emission from the device a faraday cup masked with $500 \mu\text{m}$ diameter pinhole is used. The pinhole defines the amount of ions reaching the detector and therefore controls the magnitude of the ion pulse. The energy of nitrogen ions is estimated using the time of flight technique. It is found that the ion beam signal arises due to ions having kinetic energies in the range from approximately 20 to 300 keV [16].

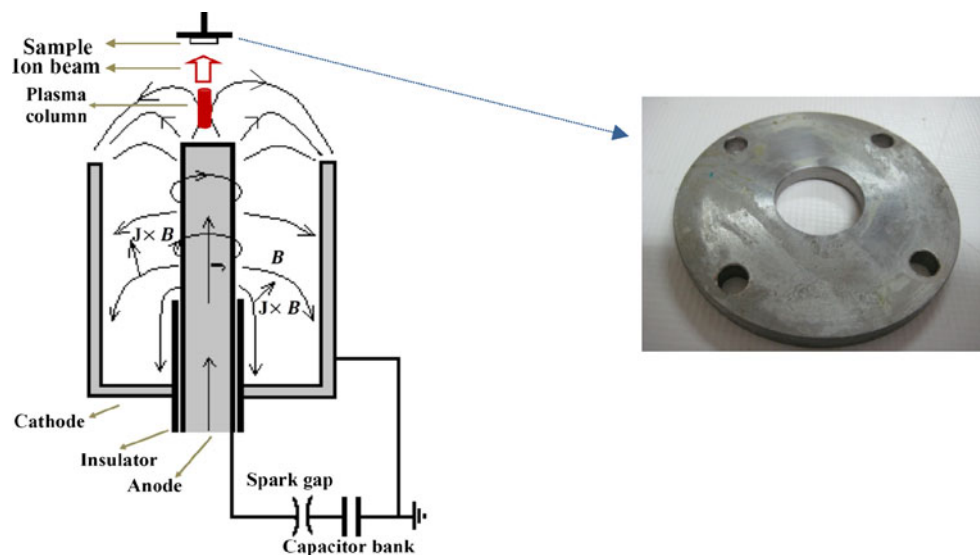
Nitrogen plasmas and their characteristics, suggest that they provide significant plasma densities and populations of reactive species for effective plasma treatments on a variety of materials [17]. As it shown in Fig. 3, the ions in the plasma help breaking C=C bonds to C–C preparing the acrylic acid to form poly acrylic acid.

In the present work, we investigated formation of ppAA by APF device. After 15 shots, nitrogen pulses performed polymerization on the specimens and the main peaks of ATR spectra assured poly acrylic acid formation on SBR substrate.

Experiments

The APF is a 4.5 kJ plasma focus of Mather type. The condenser bank consists of a single low inductance capacitor of $36 \mu\text{F}$ capacitance, 30 nH inductance, and maximum potential of about 16 kV. The measured total external inductance of the device is 115 nH [18]. A parallel plate spark gap with a swinging cascade configuration was used as a high voltage switch. The gap was triggered via an isolating capacitor using HV SCR via a T.V transformer. The experimental set up is shown in Fig. 4. The cathode is in the form of a squirrel cage consisting 6 cooper rods

Fig. 4 Sketch of APF plasma focus device



arranged concentrically around the anode with a diameter of 44.7 mm and a length of 145 mm. Anode and cathode were separated by Pyrex tube of 45 mm length. Before starting each series of discharges, a vacuum up to $\sim 5 \times 10^{-3}$ Torr is achieved with a double stage rotary pump. The gas (nitrogen) was fed to the discharge tube by using a needle valve and pressure is read with a pirani gauge.

After adjusting the working pressure, transfer of energy from the capacitor to coaxial electrodes is made by a rail gap switch. To measure the current flowing into the anode, the signal of Rogowski coil displayed on the oscilloscope.

Since the goal of this study is the formation of ppAA regardless of thickness of layers, instead of introducing acrylic acid to the chamber we carefully coat our substrate with thin layer of acrylic acid (99%, Merck KGaA). Commercial SBR substrates are cut and prepared to stand in the holder. Specimen (size $20 \times 15 \times 10$ mm 3) were introduced into the plasma focus chamber and mounted axially above the anode at a distance of 8 cm. Neither bias voltage nor auxiliary heating is applied to the specimen. Schematic diagram of plasma focus electrodes configuration is illustrated in Fig. 4.

Throughout the experiment, the filling gas pressure is kept at 2 Torr to obtain strong focusing action. The focusing efficiency is monitored using Rogowski coil, Farady cup and scintillation detector. Typical signals of current discharge, ion beam intensity and hard X-ray intensity are shown in Fig. 5. After 15 shots ppAA was produced on the substrate.

The chemical composition of plasma-polymerized coating is obtained using Fourier transform infrared spectroscopy (FTIR) on a Bruker Equinox 55 equipped with ATR accessory with 0.4 cm resolution and 32 scans for each spectrum in the range between 600 and 4,000 cm $^{-1}$.

Results and Discussion

Number of Shots

After each experimental setup substrates were washed with water to remove the non-stable and soluble compounds. One of the targets is to reduce the number shots for the formation of the ppAA for both reducing the duration of polymerization and preventing the damage to substrates. First we test with 5 shots; there was a weak ppAA layer on both steel and SBR. At this step only water contact angle and its adhesion to the surface was examined. For further plasma treatments we increased the number of pulses to 15; after this number of shots Polymerization with better characteristics on the specimens and no physical damage observed. To check the polymerization durations a comparison of plasma deposition durations in most recent devices apart from preparation of each device is shown in Table 1.

Increasing number of shots to 30 formed a more stable powder like white solid on the substrate but on the other has side effects like traces of Cu on polymer layers which reduce the quality of polymers.

ATR-FTIR Results

To confirm the polymerization of acrylic acid and before this analysis one should know assignments of FTIR-ATR of each chemical band for both before and after of polymerization of main specimen [19] (here are acrylic acid, poly acrylic acid and SBR) and also probable reaction which may occur (here poly-amides because of the presence of nitrogen ions).

Since except C=C band all other bands are the same in both acrylic and poly acrylic acid the full spectrum in

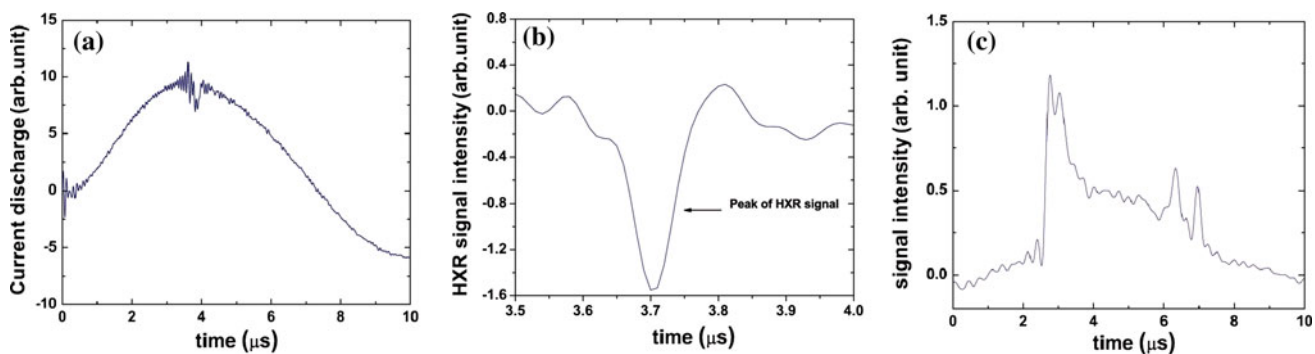


Fig. 5 Typical signals of **a** Pinched current signal, **b** Hard X-ray intensity and **c** Ion beam emission measured with farady cup placed at a distance of 8 cm in front of the anode bar (N_2 , 10 kV, 2 torr) to monitor focusing efficiency

Table 1 Comparison of deposition time in most recent devices

Device	Deposition time
Typical RF reactor	10–40 min [3, 8] ^a
DBD	2–5 min [4]
1.8 kJ plasma focus	<4 min; 30 s. For each shot

^a This data are approximate and can vary according to devices and experimental purposes and in some cases reach to 80 min [8]

Table 2 Assignments of FTIR-ATR absorption bands (excluding SBR)

Type of vibration	Wave number (cm^{-1})
OH broad band	2,800–3,500
CH stretch band	2,800–3,000
C=O	1,695–1,725
OH deformation	910–950
C=C	1,617–1,634
CH ₂ bending	1,430
C–O vibration	1,167–1,250
C–N stretch band	1,055–1,175

references would be useful [20, 21] to distinguish between them. Assignments for main absorption bands and potential C–N band are shown in Table 2. More accurate analysis can be done by knowing the peaks of each specimen using references and comparing the full spectra which are also may be available in some FTIR-ATR devices libraries. In this case we introduced some main peaks (without mentioning their band) of SBR, acrylic and poly acrylic acid in Table 3.

To investigate the uniformity of polymerization we shall discuss ATR spectrum of ppAA layers on SBR substrate at the centre and the edge of a typical substrate in Figs. 6 and 7 respectively.

In Figs. 6 and 7 some main peaks that illustrate formation of poly acrylic acid are as follows. CH stretch band

Table 3 Compounds main peaks wave number (actual data may vary, italic numbers observed) [20, 21]

Compound	Wave number (cm^{-1})
Poly acrylic acid	2940, 1715, 1420, 1400, 1250, 1190
Acrylic acid	2992, 1704, 1637, 1617, 1435, 1299, 1060, 985
SBR	2900, 2800, 1650, 1480, 1440, 960, 900, 700

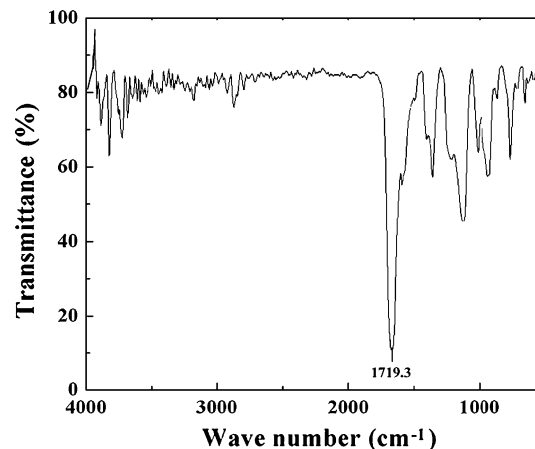


Fig. 6 ATR spectra of ppAA layers at the centre of SBR substrate

between 3,000 and 2,800 cm^{-1} which is more intensive at the edge of the substrate, CH₂ bending band approximately in 1,453 cm^{-1} at the centre and 1,442 cm^{-1} at the edge of the substrate, C–O band in about 1,173 cm^{-1} at the centre and 1,181 cm^{-1} at the edge, C=O band in about 1,719 cm^{-1} at the centre and 1,725 cm^{-1} at the edge, and small OH deformation peak in around 912 cm^{-1} for both of them. These peaks are the main peaks to assure formation of poly acrylic acid.

As it is shown there is no peak corresponding to C=C band. There are unknown peaks in around 1,060 cm^{-1} for centre and 966 cm^{-1} for the edge. The first one is due to small residuals of acrylic acid [20] as will discuss later, the latter may refer to SBR substrate because of thin polymer

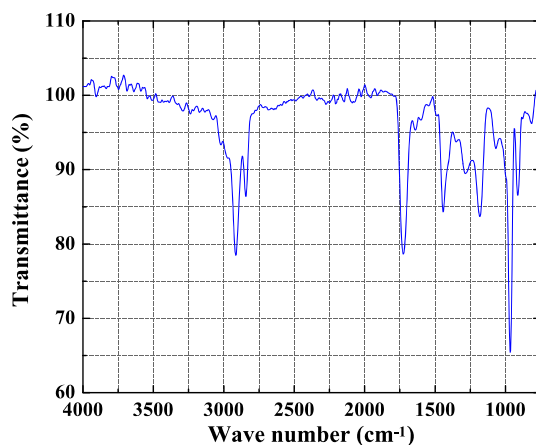


Fig. 7 ATR spectra of ppAA layers at the edge of SBR substrate

layer in a specific point and the penetration depth of ATR is greater than the polymer layer.

The C=O/CH bands ratio will help to know stability and concentration of polymers by calculating the areas of each band. This amount is about 1.4 in off centre and 9 in the centre. While C=O/CH bands ratio in the edge is comparable with those obtained in [3, 9] this amount in centre is extraordinary high. This may refer to the limitation of our setup that instead of introducing aerosols, substrates were coated with acrylic acid and the effect of gravity does not let acrylic acid layer to spread in the same thickness over the layer and during the polymerization some acid under polymer layer will be detected in infra red spectra and or may there exists a traces of acrylic acid. However, to assure the formation of polymer in the centre, the centre spectra is checked with device ATR library in Fig. 8 which is well matched. Geometry of plasma focus electrodes and the holder against gravity direction lead to non uniform spread of acrylic acid on the substrates. This effect results to detection of some acrylic acid layers under polymer layers. However, as it shown in Fig. 8, to assure the formation of polymer, experimental spectrum of specimen at the center is checked with ATR library.

Conclusions

This paper provides new information about formation of plasma polymer acrylic acid by APF device. Setting the device for most optimum ion characteristics lead us to plasma polymer acrylic acid after few shots on discharge energy of about 1.8 kJ. Optimum number of shots to achieve stable polymers without side effects is one of the concerns. Styrene-Butadiene-Rubber used as substrate and nitrogen puffed into the chamber as medium gas. After 15 shots, nitrogen pulses performed polymerization on the specimens and the main peaks of ATR spectra assured poly-

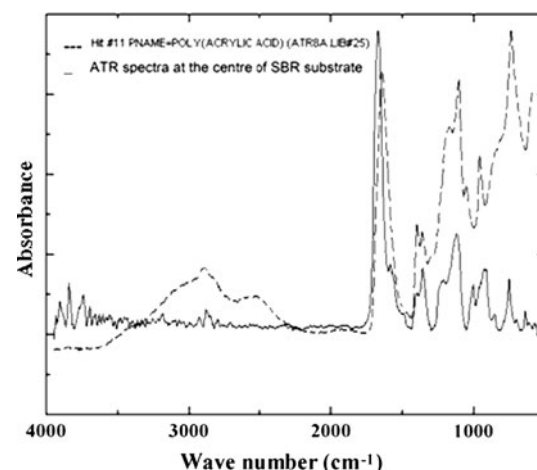


Fig. 8 Comparison of experimental spectrum of specimen at the centre with one obtained from ATR device library

acrylic acid formation on SBR substrate. Increasing the plasma treatments to more than 30 shots give an enhanced adhesion and sputtered Cu layers on SBR substrate observed.

References

- D. Hegemann, E. Korner, S. Guimond, *Plasma Process. Polym.* **6**, 254 (2009)
- R.D. Short, D.A. Steele, *Plasma Process. Polym.* **7**, 370 (2010)
- S. Zanini, R. Ziano, C. Riccardi, *Plasma Chem. Plasma Process.* **29**, 535 (2009)
- R. Morent, N. De Geyter, S. Van Vlierberghe et al., *Plasma Chem. Plasma Process.* **29**, 103 (2009)
- M.M. Pastor-Blas, J.M. Martin-Martinez, G.J. Dillard, *Surf. Interface Anal.* **26**, 385 (1998)
- G. Martinez Delfa, A. Olivieri, C.E. Boschetti, *Comput. Chem. Eng.* **33**, 850 (2009)
- V. Sciarattta, U. Vohrer, D. Hegemann et al., *Surf. Coatings Technol.* **174**, 805 (2003)
- B. Gupta, S. Saxena, A. Ray, *J. Appl. Polym. Sci.* **107**, 324 (2008)
- Z. Jiang, Z.J. Jiangb, Y. Shi et al., *Appl. Surf. Sci.* **256**, 6473 (2010)
- F. Basarir, E.Y. Choi, S.H. Moon et al., *J. Membr. Sci.* **260**, 66 (2005)
- J.W. Mather, *Phys. Fluid* **8**(2), 366 (1965)
- J.W. Mather, *Methods of Experimental Physics* (Academic Press, New York, 1971)
- M.P. Srivastava, S.R. Mohanty, S. Annapoorni et al., *Phys. Lett. A* **215**, 63 (1996)
- J. Piekoszewski et al., *J. Appl. Phys.* **64**, 2648 (1988)
- W. Stygar, G. Gerdin, F. Venneri et al., *Nucl. Fusion* **22**, 1161 (1982)
- S. Mehboob, S. Ahmad, A. Waheed et al., *Plasma Sources Sci. Technol.* **15**, 295 (2006)
- J.M. Grace, L.J. Gerenser, *J. Dispers. Sci. Technol.* **24**(3), 305 (2003)
- M. Habibi, R. Amrollahi, M. Attaran, *J. Fusion Energ.* **28**, 130 (2009)

19. L.J. Bellamy, *The Infra-Red Spectra of Complex Molecules* (Chapman and Hall, London, 1975)
20. C.J. Pouchert, *The Aldrich library of infrared spectra* (Aldrich Chemical Co., Milwaukee, 1981)
21. K.G.R. Pachler, F. Matlok, H.U. Gremlich, *Merck FT-IR Atlas: A Collection of FT-IR Spectra* (VCH, Weinheim, New York, 1988)